

complex was prepared by a published procedure.¹

[2,3,11,12,14,20-Hexamethyl-3,11,15,19,22,26-hexaazatricyclo-[11.7.7.1^{5,9}]octacos-1,5,7,9(28),12,14,19,21,26-nonaene-κ⁴N]nickel(II) Hexafluorophosphate (II). This complex was prepared by a published procedure.⁸

[2,12,14,20-Tetramethyl-3,11,15,19,22,26-hexaazatricyclo-[11.7.7.1^{5,9}]octacos-1,5,7,9(28),12,14,19,21,26-nonaene-κ⁴N]nickel(II) Hexafluorophosphate (III). This complex was prepared by published procedures and carefully purified to ensure no dimer was present.⁸

(5R*,9S*)-[2,12,14,20-Tetramethyl-3,11,15,19,22,26-hexaazatricyclo-[11.7.7.1^{5,9}]octacos-1,12,14,19,21,26-hexaene-κ⁴N]nickel(II) Hexafluorophosphate (IV). This complex was prepared by published methods.¹⁹

[2,9,10,17,19,25,33,34-Octamethyl-3,6,13,16,20,24,27,31-octaazapentacyclo[16.7.7.2^{8,11}.2^{3,6}.2^{13,16}]octatriaconta-1,8,10,17,19,24,26,31,33-nonaene-κ⁴N]nickel(II) Hexafluorophosphate (V). This complex was also prepared by published methods.⁴

Physical Measurements. Proton NMR spectra were acquired by using Bruker WM300, Bruker AM500, and Nicolet NT500 spectrophotometers. All NMR spectra were obtained in acetonitrile-*d*₃. The ¹H-¹³C shift correlation measurements were acquired on a Bruker WM300 spectrometer with SI = 4K, TD₁ = 256, P₉₀H = 44 μs, and P₉₀C = 29 μs. The 2-D NOESY and COSY experiments were acquired on a Bruker AM500 with the Bruker COCO-NOESY Shift-Correlated 2-D sequence

with a 0.5-s mixing time. The SW = 4000 Hz and SI = 16K. This program allows for the COSY data to be acquired during the mixing time and has been adapted from Haasnoot et al.^{22,23} The ¹³C DEPT experiments were carried out on a Bruker NR-80 spectrophotometer with a sweep width of 4500 Hz and PW = 35 μs; the data were acquired over 16K data points.

Acknowledgment. We wish to thank Dr. Colin J. Cairns for providing complex III and Dr. Dennis L. Nosco for providing complex IV. The financial support of the U.S. National Institutes of Health, Grant No. GM10040, and of the U.S. National Science Foundation, Grant No. CHE-8402153, is greatly appreciated. FT-NMR spectra at 11.75 T (500 MHz) and 7.0 T (300 MHz) were obtained at The Ohio State University Chemical Instrument Center by using equipment funded in part by NIH Grant No. 1 S10 RR01458-01A1.

Registry No. I, 73914-16-6; II, 77827-37-3; III, 77827-31-7; IV, 110796-22-0; V, 85630-88-2.

(22) Haasnoot, C. A. G.; Van De Ven, F. J. M.; Hilbers, C. W. *J. Magn. Reson.* **1984**, *56*, 343.

(23) Gurevich, A. Z.; Barsukov, I. L.; Arseniev, A. S.; Bystrov, V. F. *J. Magn. Reson.* **1984**, *56*, 471.

Contribution from the Instituto de Quimica, Universidade de Sao Paulo, CP 20780, Sao Paulo, SP, Brazil, and Department of Chemistry, York University, North York, Ontario, Canada M3J 1P3

Binding of Pentaammineruthenium(II) Residues to the Tris(bipyrazine)ruthenium(II) Cation

Henrique E. Toma,*^{1a} Pamela R. Auburn,^{1b} Elaine S. Dodsworth,^{1b} M. Neal Golovin,^{1b} and A. B. P. Lever*^{1b}

Received November 21, 1986

A series of [(NH₃)₅Ru]_n(bpz)]²ⁿ⁺ (bpz = bipyrazine; *n* = 1, 2) and [Ru(bpz)₃][Ru(NH₃)₅]_n⁽²⁺²ⁿ⁾⁺ (*n* = 1, 3, 6) complexes have been synthesized and characterized by means of electronic spectra, ¹H NMR spectroscopy, cyclic voltammetry, and spectroelectrochemistry. The complexes are very stable and inert in aqueous solution. The peripheral pentaammineruthenium(II) groups in the tris(bipyrazine) series exhibit strong absorption bands in the visible region, around 490 and 660 nm, ascribed to metal-to-ligand charge transfer transitions. The attached ions can be reversibly oxidized, with formal potentials of approximately 0.65 V versus NHE, in comparison to 0.52 V for the [(NH₃)₅Ru]_n(bpz)]²ⁿ⁺ complexes. No evidence of intervalence bands with ε > 100 M⁻¹ cm⁻¹ has been observed in the near-IR region of mixed-valence species. The spectroscopic and electrochemical data are consistent with a very weak interaction between the peripheral pentaammineruthenium(II) groups.

Introduction

Ruthenium(II) complexes of bipyrazine (bpz) are of special interest in coordination chemistry, because of their pronounced photochemical activity and of the existence of six peripheral nitrogen atoms available to bind Lewis acids and transition-metal ions.²⁻¹⁰ Recently, we reported a detailed kinetic and spectroscopic study on a series of di- to heptanuclear tris(bipyrazine)ruthenium(II) pentacyanoferrate(II) complexes in aqueous solution.¹¹ In this work, we extend the investigation to a series of pentaammineruthenium(II) derivatives, including the [Ru(NH₃)₅-

(bpz)]²⁺ and [Ru(NH₃)₅]₂(bpz)]⁴⁺ species in solid state and in aqueous solution. Electrochemical and electronic spectroscopic data reveal that the several pentaammineruthenium(II) groups are essentially uncoupled to one another and to the central ruthenium atom.

Experimental Section

The bipyrazine ligand was prepared by the pyrolysis of the bis(2-pyrazinecarboxylato)copper(II) complex at 270–290 °C, under an argon atmosphere, as described in the literature.^{3,12} The solid was recrystallized from toluene, yielding pale yellow crystals, mp 186–190 °C (lit.¹³ mp 190 °C).

The complexes [Ru(bpz)₃](PF₆)₂ and [Ru(NH₃)₅(H₂O)](PF₆)₂ were prepared by literature methods.^{2,14} [Ru(NH₃)₅(bpz)](PF₆)₂ and [Ru(NH₃)₅]₂(bpz)](PF₆)₄ were obtained by reacting 0.20 mmol of bpz with 0.20 or 0.40 mmol of [Ru(NH₃)₅(H₂O)](PF₆)₂ in boiling acetone (25 mL) under an argon atmosphere. After 30 min, the deep purple solution was evaporated to dryness at 55 °C under a vigorous stream of argon. The black residue was kept under vacuum for 1 day and then washed with toluene. The compounds were recrystallized by dissolving in a small volume of 1:1 water-acetone solution and allowing the solvent to evaporate very slowly under reduced pressure. Anal. Calcd for [Ru(NH₃)₅(bpz)](PF₆)₂: C, 15.15; H, 3.33; N, 19.87. Found: C, 14.6; H, 3.2; N, 19.7. Calcd for [Ru(NH₃)₅]₂(bpz)](PF₆)₄·C₃H₆O: C, 11.31; H,

- (1) (a) Universidade de Sao Paulo. (b) York University.
- (2) Crutchley, R. J.; Lever, A. B. P. *J. Am. Chem. Soc.* **1980**, *102*, 7128.
- (3) (a) Crutchley, R. J.; Lever, A. B. P. *Inorg. Chem.* **1982**, *21*, 2276. (b) Crutchley, R. J.; Kress, N.; Lever, A. B. P. *J. Am. Chem. Soc.* **1983**, *105*, 1170.
- (4) Rillema, D. P.; Allen, G.; Meyer, T. J.; Conrad, D. *Inorg. Chem.* **1983**, *22*, 1617.
- (5) Crutchley, R. J.; Lever, A. B. P.; Poggi, A. *Inorg. Chem.* **1983**, *22*, 2647.
- (6) Gonzales-Velasco, J.; Rubinstein, I.; Crutchley, R. J.; Lever, A. B. P.; Bard, A. J. *Inorg. Chem.* **1983**, *22*, 822.
- (7) Dodsworth, E. S.; Lever, A. B. P. *Chem. Phys. Lett.* **1984**, *112*, 567.
- (8) Dodsworth, E. S.; Lever, A. B. P.; Eryavec, G.; Crutchley, R. J. *Inorg. Chem.* **1985**, *24*, 1906.
- (9) Haga, M.-A.; Dodsworth, E. S.; Eryavec, G.; Seymour, P.; Lever, A. B. P. *Inorg. Chem.* **1985**, *24*, 1901.
- (10) Balk, W. R.; Stufkens, D. J.; Crutchley, R. J.; Lever, A. B. P. *Inorg. Chim. Acta* **1982**, *64*, L49–50.
- (11) Toma, H. E.; Lever, A. B. P. *Inorg. Chem.* **1986**, *25*, 176.

(12) Lafferty, J. J.; Case, F. H. *J. Org. Chem.* **1967**, *32*, 1591.

(13) Lever, A. B. P.; Lewis, J.; Nyholm, R. S. *J. Chem. Soc.* **1964**, 1187.

(14) Kuehn, C. G.; Taube, H. *J. Am. Chem. Soc.* **1976**, *98*, 689.

Table I. Visible-UV Spectral Data for Ruthenium(II)-Bipyrazine-Ruthenium(II)-Ammine Polynuclear Complexes^a

species	peripheral MLCT		central MLCT		internal $\pi \rightarrow \pi^*$ and high-energy MLCT bands	
bpz ^b					288 (4.29)	227 (4.02)
[Ru(bpz) ₃] ²⁺ ^c			442 (4.18)	342 (4.27)	295 (4.79)	241 (4.37)
					266 (4.34)	
[Ru(NH ₃) ₅ (bpz)] ²⁺	500 (3.81)				288 (4.04)	228 (3.86)
[Ru(NH ₃) ₅ (bpzH)] ³⁺	569 (3.81)	430 (sh)			310 (3.90)	238 (3.89)
[(NH ₃) ₅ Ru] ₂ (bpz)] ⁴⁺	508 (4.20)				288 (4.14)	227 (4.06)
[(NH ₃) ₅ Ru] ₂ (bpzH)] ⁵⁺	572 (4.08)	440 (sh)			310 (4.04)	240 (4.00)
[Ru(bpz) ₃ Ru(NH ₃) ₅] ⁴⁺	654 (3.81)	490 (sh)	442 (4.11)	340 (sh)	296 (4.66)	238 (4.32)
			415 (sh)		263 (sh)	
[Ru(bpz) ₃ Ru(NH ₃) ₅] ⁸⁺	664 (4.40)	490 (4.32)	masked		300 (4.68)	238 (4.43)
					260 (sh)	
[Ru(bpz) ₃ Ru(NH ₃) ₅] ¹⁴⁺	672 (4.77)	490 (4.64)	masked		302 (4.66)	240 (4.50)
					262 (sh)	

^aAll data were recorded in aqueous solution, except where indicated, and are in nanometers (log ϵ in parentheses). ^bIn ethanol; ref 3. ^cIn acetonitrile; ref 3.

3.62; N, 16.78. Found: C, 11.0; H, 3.6; N, 15.8.

The polynuclear complexes [Ru(bpz)₃[Ru(NH₃)₅] _{π}]^{(2+2 π)⁺ ($\pi = 1, 3, 6$) were synthesized by reacting 0.025 mmol of [Ru(bpz)₃](PF₆)₂ with 0.025, 0.075, or 0.150 mmol of [Ru(NH₃)₅(H₂O)](PF₆)₂ in boiling acetone (25 mL) under an argon atmosphere. After 30 min, the violet-blue solution was evaporated to dryness, at 55 °C, with a vigorous stream of argon. Recrystallization was carried out as in the preceding examples. Anal. Calcd for [Ru(bpz)₃Ru(NH₃)₅](PF₆)₄: C, 21.48; H, 2.48; N, 17.74. Found: C, 21.6; H, 3.0; N, 17.9. Calcd for [Ru(bpz)₃[Ru(NH₃)₅]₃](PF₆)₈: C, 12.56; H, 2.76; N, 16.49. Found: C, 12.7; H, 2.9; N, 15.5. Calcd for [Ru(bpz)₃[Ru(NH₃)₅]₆](PF₆)₁₄: C, 7.74; H, 2.92; N, 15.79. Found: C, 8.1; H, 3.0; N, 15.2.}

The electronic spectra in the visible-UV region were recorded on a Hewlett-Packard 8451-A diode-array spectrophotometer. The absorption spectra in the near-infrared region were obtained with a Cary 17 spectrophotometer, with the samples dissolved in D₂O. Nuclear magnetic resonance spectra were recorded on a Varian T-60 spectrometer, at a probe temperature of 33 °C. The measurements were made in D₂O, with use of 0.03–0.05 M solutions, after converting the hexafluorophosphate salts into the more soluble chloride form, with tetraphenylarsonium chloride. The chloride salts can also be obtained by dissolving the hexafluorophosphate compounds in acetone and adding one or two drops of concentrated hydrochloric acid. The chloride salts precipitate almost quantitatively in the presence of acetone and can easily be separated by filtration. Data were collected in the presence of 0.1 M methanol as internal calibrant and converted to the TMS scale by using 3.47 ppm for CH₃.

Cyclic voltammetry was carried out with Princeton Applied Research Corp. (PARC) instrumentation, consisting of a Model 173/179 potentiostat and a Model 175 universal programmer. A glassy-carbon electrode was employed for the measurements in aqueous solution, with use of a conventional Luggin capillary arrangement with a Ag/AgCl (1 M KCl) reference electrode. A platinum wire was used as the auxiliary electrode. The measured potentials were converted to the NHE scale by adding 0.222 V. For the measurements in acetonitrile solutions, a platinum-disk electrode was used versus a Ag/Ag⁺ (0.01 M silver nitrate in acetonitrile) reference electrode in the presence of 0.10 M tetraethylammonium perchlorate ($E^\circ = 0.503$ vs NHE).¹⁵ For the spectroelectrochemical measurements, the PARC Model 173/179 potentiostat was used in parallel with the Cary 17 or HP 8451-A spectrophotometer. A three-electrode system was designed for a rectangular quartz cell of 0.030-cm optical path length. A gold minigrad was used as a transparent working electrode, in the presence of a small Ag/AgCl reference electrode and a platinum auxiliary electrode.

Results and Discussion

The electronic spectra of the [Ru(NH₃)₅(bpz)]²⁺ and [[Ru(NH₃)₅]₂(bpz)]⁴⁺ complexes are illustrated in Figure 1. The absorption bands at 230 and 286 nm also occur in free bpz and are ascribed to internal $\pi \rightarrow \pi_2^*$ and $\pi \rightarrow \pi_1^*$ transitions in the aromatic ligand, respectively. The absorption band around 500 nm is assigned to the Ru(π) \rightarrow bpz(π_1^*) charge-transfer (MLCT) transition, by comparison with the spectra of pentaammine-ruthenium(II) complexes of aromatic N-heterocycles.¹⁶ A second

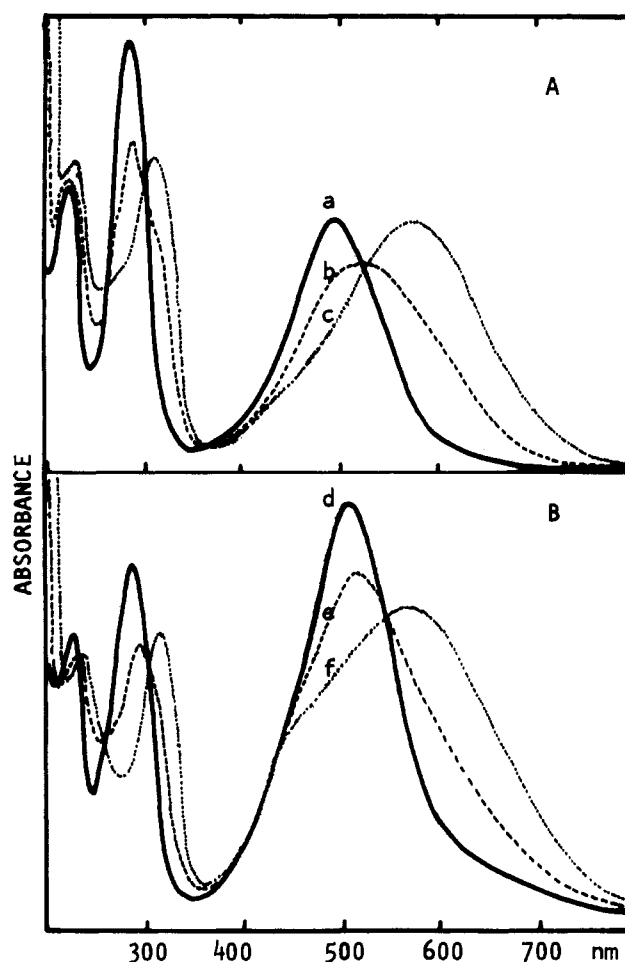


Figure 1. Electronic spectra of (A) [Ru(NH₃)₅(bpz)]²⁺ and (B) [[Ru(NH₃)₅]₂(bpz)]⁴⁺ (0.05 mM) in (a, d) water (pH 7), (b, e) 0.12 M HCl, and (c, f) 3 M HCl.

MLCT band associated with the Ru(π) \rightarrow bpz(π_2^*) transition is expected in a cis (bipyrazine)metal complex at a wavenumber approximately 8×10^3 cm⁻¹ higher than that of the first one, i.e. around 360 nm. This band was not observed in either species, and its absence may be evidence of a trans configuration for these species. The UV $\pi \rightarrow \pi^*$ transitions (Table I) in these species lie at the same energies as in the free (trans) ligand and differ in both position and separation from those obtained for the cis bidentate species. A summary of the electronic transitions can be

(15) Kratochvil, B.; Lorah, E.; Garber, C. *Anal. Chem.* **1969**, *41*, 1793.

(16) Ford, P.; Rudd, D. F. P.; Gaunder, R.; Taube, H. *J. Am. Chem. Soc.* **1968**, *90*, 1187.

seen in Table I. While both the 1:1 and 2:1 species can theoretically exist in several isomeric forms depending upon which bpz nitrogen atoms are involved, the clarity of the NMR and UV/vis spectra lead one to believe that only one isomer is present in each case. On the basis of minimizing steric hindrance, binding only to N4 is most likely (see labeling in Figure 4), and will be assumed henceforth. Note that neither the ^1H NMR nor the UV spectrum of the 1:1 adduct is consistent with the alternative formulation of this species with a bidentate bipyrazine ligand, i.e. as $[\text{Ru}(\text{NH}_3)_4(\text{bpz})]^{2+}$.

Protonation of the pentaammineruthenium(II)-bipyrazine complexes leads to a bathochromic shift of the $\pi-\pi^*$ and MLCT bands, with several isosbestic points in the visible and UV regions, as shown in Figure 1.

Quantitative measurements using freshly prepared solutions were carried out rapidly in order to minimize the acid-catalyzed aquation of the ruthenium(II) ammines.¹⁷ In 0.01–6 M HCl solutions, a single protonation equilibrium is involved in the complexes. The corresponding $\text{p}K_a = 0.85 (\pm 0.05)$ for both the mononuclear and binuclear complexes was calculated from the linear plots of pH versus $\log [(A - A_i)/(A_f - A)]$, where A is absorbance and the subscripts i and f refer to the initial and final solutions, respectively. A slope of unity was observed, in agreement with the single-protonation hypothesis.¹⁸ The similar $\text{p}K_a$'s of the mononuclear and binuclear complexes are consistent with protonation at the free N atom of the coordinated pyrazine ring. This atom is expected to have its basicity increased by the back-bonding interactions from the Ru(II) ion. In accordance, the $\text{p}K_a$ values of the complexes are higher than that previously reported for the free bpz ligand ($\text{p}K_a = 0.45$).³ The increase in basicity of the peripheral nitrogen atom of the coordinated ring is very small, certainly far smaller than the increase observed in $[(\text{NH}_3)_5\text{Ru}(\text{pyz})]^{2+}$ (pyz = pyrazine) when it is protonated (from 0.6 to 2.5)¹⁹ or 2,6-dimethylpyrazine (from 1.94 to 3.70).¹⁸ Possibly the existence of the $\text{N}=\text{C}-\text{C}=\text{N}$ framework created in the bipyrazine system generates an alternate path for delocalization such that the basicity of the far nitrogen is not greatly enhanced (vide infra). Approximate values for the excited-state $\text{p}K_a$'s were calculated on the basis of eq 1, excepting, however,

$$\text{p}K_a^* = \text{p}K_a(\text{gs}) + (\nu_1 - \nu_2)/476.5 \quad (1)$$

that such values are approximate, especially if there is excited-state structural distortion or solvent-dipole-induced distortion.^{19,20} In the case of the mononuclear complex, $\nu_1 = 20000 \text{ cm}^{-1}$, $\nu_2 = 17580 \text{ cm}^{-1}$ and $\text{p}K_a^* = 5.9$. In the case of the binuclear complex, $\nu_1 = 19700 \text{ cm}^{-1}$, $\nu_2 = 17480 \text{ cm}^{-1}$, and $\text{p}K_a^* = 5.5$. The value of $\text{p}K_a^*$ is some 2 pK units less than for the pyrazine complex but the difference $\text{p}K_a - \text{p}K_a^*$ is actually rather larger, in both complexes, for the bipyrazine system than for the pyrazine system (5.05 and 4.65 vs 3.9 units)¹⁹ but less than the difference (5.95 units) seen with the 2,6-dimethylpyrazine system.¹⁸ This discussion must be tempered with the suspicion that the unprotonated species has a trans bpz group, while, possibly, either of the two protonated species in question may be cis.

Further protonation of the complexes can be observed in concentrated sulfuric acid; however, accurate measurements were precluded by the rapid decomposition of the complexes.

The electronic spectra of the $[\text{Ru}(\text{bpz})_3\{\text{Ru}(\text{NH}_3)_5\}_n]^{(2+2n)+}$ complexes ($n = 1, 3, 6$) can be seen in Figure 2. The absorption bands around 230, 260, 300, 340, and 440 nm were also observed in the $[\text{Ru}(\text{bpz})_3]^{2+}$ cation. The last two bands were ascribed³ to the $\text{Ru}_c(\pi) \rightarrow \text{bpz}(\pi_2^*)$ and $\text{Ru}_c(\pi) \rightarrow \text{bpz}(\pi_1^*)$ MLCT transitions (subscript c refers to central), respectively. Two additional bands appearing around 490 and 660 nm in the spectra of the polynuclear complexes exhibit intensities that increase with the number of attached $[\text{Ru}(\text{NH}_3)_5]^{2+}$ groups (Table I). The energy difference of 5300 cm^{-1} is comparable to that observed for the MLCT bands of the $[\text{Ru}(\text{bpz})_3]^{2+}$ complex, and these new

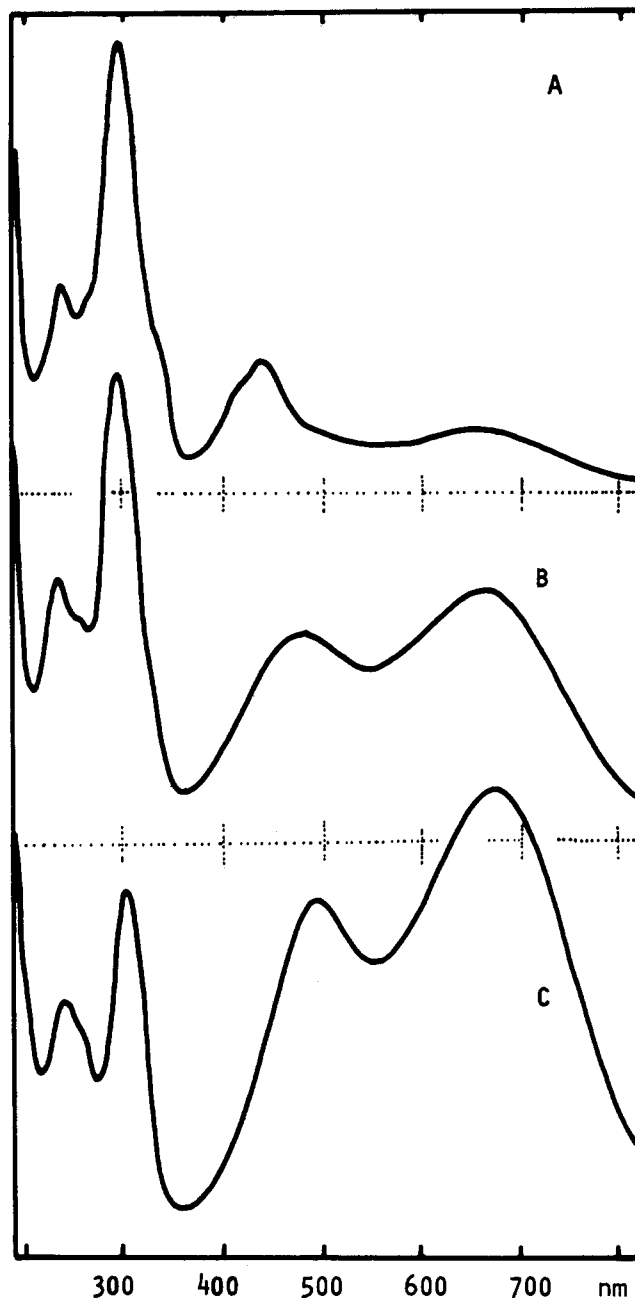


Figure 2. Electronic spectra of the $[\text{Ru}(\text{bpz})_3\{\text{Ru}(\text{NH}_3)_5\}_n]^{(2+2n)+}$ polynuclear complexes in aqueous solution with $n = 1$ (A), 3 (B), and 6 (C), around 0.037, 0.033, and 0.017 mM, respectively.

bands can be assigned to the $\text{Ru}_p(\pi) \rightarrow \text{bpz}(\pi_2^*)$ and $\text{Ru}_p(\pi) \rightarrow \text{bpz}(\pi_1^*)$ MLCT transitions from the peripheral (p) metal ions, respectively. In Figure 3 one can see two different aspects associated with the presence of free peripheral N atoms in the $[\text{Ru}(\text{bpz})_3\{\text{Ru}(\text{NH}_3)_5\}_3]^{8+}$ complex. First, the complex can be protonated in concentrated HCl, with a set of four simultaneous isosbestic points, and $\text{p}K_a = -2.1$. This value has been evaluated from the H_0 acidity functions for concentrated HCl solutions²¹ and can be compared with the $\text{p}K_a = -2.2$ of the $[\text{Ru}(\text{bpz})_3]^{2+}$ complex.^{3b} In the presence of concentrated sulfuric acid, further changes are observed in the spectra that seem to indicate more drastic effects in the structure of the complexes. The possibility of decomposition reactions cannot be excluded in this case. The red-shifted absorption can be assigned to a transition of the type $\text{Ru}(\pi) \rightarrow \text{bpzH}^+(\pi^*)$, as discussed previously.^{3b} The second aspect illustrated in Figure 3B refers to the binding of $[\text{Fe}(\text{CN})_5]^{3-}$ groups in the $[\text{Ru}(\text{bpz})_3\{\text{Ru}(\text{NH}_3)_5\}_3]^{8+}$ complex.¹¹ The successive at-

(17) Ford, P. C.; Kuempel, J. R.; Taube, H. *Inorg. Chem.* **1968**, *7*, 1976.

(18) Toma, H. E.; Stadler, E. *Inorg. Chem.* **1985**, *24*, 3085.

(19) Johnson, C. R.; Shepherd, R. E. *Inorg. Chem.* **1983**, *22*, 1117.

(20) Jackson, G.; Porter, G. *Proc. R. Soc. London, A* **1961**, *260*, 13.

(21) Long, F. A.; Paul, M. A. *Chem. Rev.* **1957**, *57*, 1.

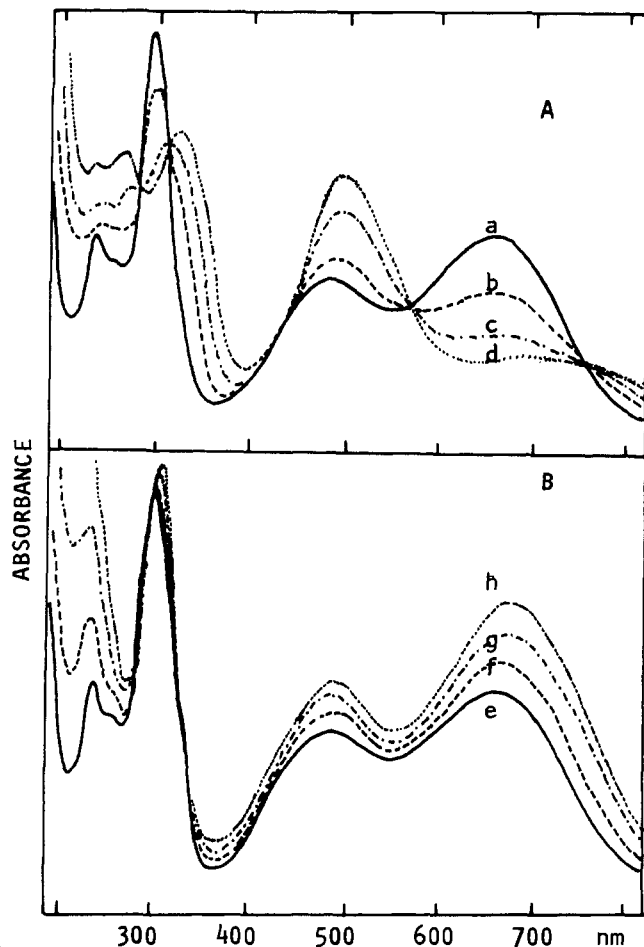


Figure 3. Electronic spectra of the $[\text{Ru}(\text{bpz})_3\{\text{Ru}(\text{NH}_3)_5\}]^{18+}$ complex (0.033 mM) (A) in (a) water (pH 7), (b) 5 M HCl, (c) 8 M HCl, and (d) 12 M HCl and (B) in the presence of (e) 0, (f) 1, (g) 2, and (h) 3 equiv of the aquapentacyanoferrate(II) ion.

tachments of one to three pentacyanoferrate(II) groups increase the intensity of the MLCT bands at 490 and 660 nm, with a small bathochromic shift (Table I). The $\text{Fe}(\pi) \rightarrow \text{bpz}(\pi^*)$ and $\text{Fe}(\pi) \rightarrow \text{bpz}(\pi_1^*)$ transitions in the series of $[\text{Ru}(\text{bpz})_3\{\text{Fe}(\text{CN})_5\}_n]^{(3n-2)+}$ complexes ($n = 1-6$) were observed near 500 and 700 nm.¹¹ Therefore, in the mixed polynuclear complexes, these bands should occur superimposed upon those from the peripheral ruthenium(II) ions. The spectrum of the $[\text{Ru}(\text{bpz})_3\{\text{Ru}(\text{NH}_3)_5\}]^{14+}$ complex is not modified by the presence of cyanoferrate(II) ions, excluding the possibility that the changes illustrated in Figure 3B arise from outer-sphere association. The assignments of the three charge-transfer bands in the visible region, described here, are fully supported by resonance Raman data, which will be discussed in detail elsewhere.²²

NMR Spectra. ^1H NMR spectra of the $[\text{Ru}(\text{NH}_3)_5(\text{bpz})]^{2+}$ and $[\{\text{Ru}(\text{NH}_3)_5\}_2(\text{bpz})]^{4+}$ complexes are shown in Figure 4B,C, in comparison with the spectrum of the free ligand (Figure 4A). The NMR peaks at 9.46 and 8.86 ppm in the free ligand have been assigned to the protons H3 and to the pair of protons H5 and H6, respectively. The NMR spectrum of the $[\text{Ru}(\text{NH}_3)_5(\text{bpz})]^{2+}$ complex exhibits an apparent doublet at 9.41 ppm, a singlet peak at 8.83 ppm, and a doublet signal at 8.27 ppm, having relative intensities of 2:3:1, respectively. The binding of $[\text{Ru}(\text{NH}_3)_5]^{2+}$ ions to the N-heterocyclic ligands has been reported²³ to produce a shielding effect at the ortho protons (here denoted as H3 and H5), as a consequence of the paramagnetic anisotropy and back-bonding interactions that predominate over the inductive effects from the Ru(II) ion. These effects have already been

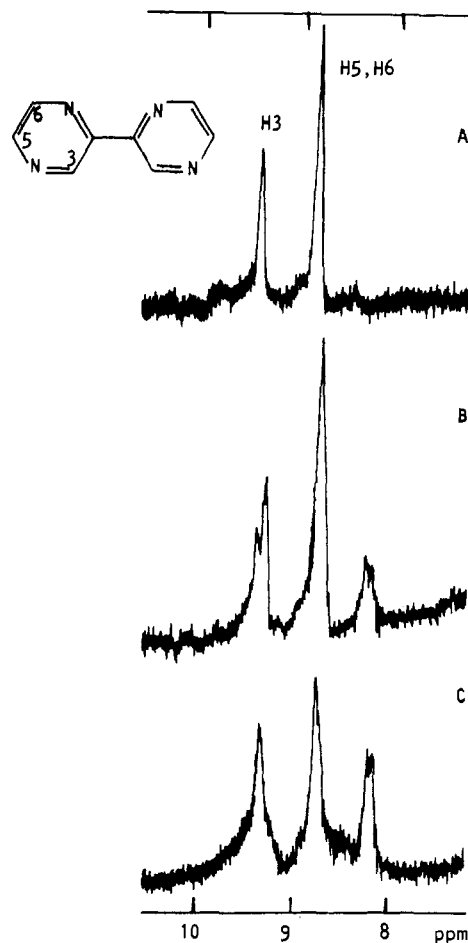


Figure 4. ^1H NMR spectra of (A) bpz, (B) $[\text{Ru}(\text{NH}_3)_5(\text{bpz})]^{2+}$, and (C) $[(\text{NH}_3)_5\text{Ru}-\text{bpz}-\text{Ru}(\text{NH}_3)_5]^{4+}$, 0.03–0.05 M in D_2O , at 30 °C (chemical shifts versus TMS).

discussed in the literature.^{3,9,11,23-25} The chemical shifts will depend on the extent of the shielding effects from π back-bonding and of the deshielding, inductive effects from the metal ion. Previously,¹¹ the H6 protons shifted upfield, while the H5 protons shifted downfield, but to a lesser extent, upon coordination by the pentacyanoferrate(II) group. Therefore, the apparent doublet at 9.4 ppm in the monomeric pentaammineruthenium(II)-bipyrazine complex can be ascribed to the nonequivalent H3 and H3' protons. The singlet peak at 8.83 ppm is associated with the remote H5', H6', and H5 protons. The new doublet at 8.27 ppm is shifted upfield (shielding), being consistent with the H6 resonance signals. The NMR spectrum of the binuclear complex is shown in Figure 4C. In this case, the pairs of H3/H3', H5/H5', and H6/H6' protons are equivalent and the three resonance signals have the same intensity.

A potential problem in discussing the NMR spectra of the $[\text{Ru}(\text{bpz})_3\{\text{Ru}(\text{NH}_3)_5\}_n]^{(2+2n)+}$ species is the probable presence of structural isomers for certain values of n . Thus, for example, for $n = 2$, two pentaammineruthenium groups may bind to different bpz ligands or, conceivably, to the same bpz ligand. Moreover, even where they bind to different bpz ligands, two isomers exist, differing in the relative positions of the pentaammine groups. We discuss here the low-field NMR considering the different types of proton present without considering their relative numbers, which will depend upon the isomer mix.

The methods used to prepare these compounds might be expected to yield a statistical mixture of products. Analytical data suggest but do not provide definitive proof of the unique n value of each species isolated. On the basis of the NMR data reported

(22) Toma, H. E.; Santos, P. S.; Lever, A. B. P., to be submitted for publication in *Inorg. Chem.*

(23) Lavalley, D. K.; Fleischer, E. B. *J. Am. Chem. Soc.* **1972**, *94*, 2583.

(24) Foust, R. D.; Ford, P. C. *J. Am. Chem. Soc.* **1972**, *94*, 5686.

(25) Lytle, F. E.; Petrosky, L. M.; Carlson, L. R. *Anal. Chim. Acta* **1971**, *57*, 239.

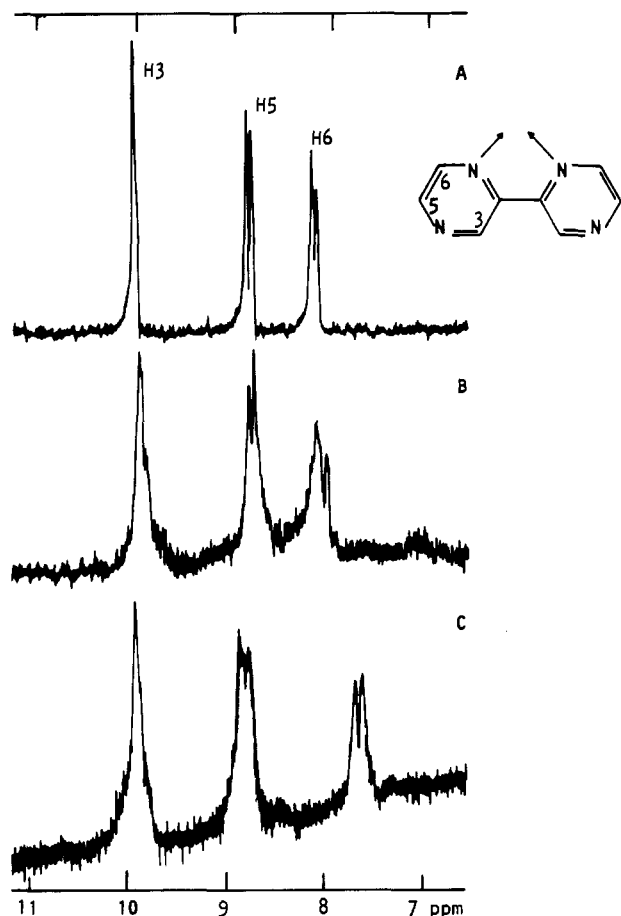


Figure 5. ^1H NMR spectra of (A) $[\text{Ru}(\text{bpz})_3]^{2+}$, (B) $[\text{Ru}(\text{bpz})_3][\text{Ru}(\text{NH}_3)_5]^{8+}$, and (C) $[\text{Ru}(\text{bpz})_3][\text{Ru}(\text{NH}_3)_5]_6^{14+}$, 0.03 M in D_2O , at 30 $^\circ\text{C}$ (chemical shifts versus TMS).

here and some preliminary high-field NMR experiments, the following statements may be made: (i) Mixing of the $n = 1$ and 3 or $n = 0$ and 6 species causes no reequilibration below 50 $^\circ\text{C}$ in water, the mixed (not averaged) spectra being obtained. (ii) The $n = 1$ species appears to be a single compound, but the presence of some $n = 0$ species cannot be ruled out. Higher values of n are absent. (iii) The $n = 3$ species spectrum is complex, indicative at least of several $n = 3$ isomers. If $n = 4-6$ species are present, they can only be present in small amounts. (iv) The $n = 6$ species is not contaminated with $n = 0-3$ species, but the presence of small amounts of $n = 4$ and 5 species cannot be excluded at this time. The evidence would indeed favor the isolation of compounds of unique n , as was apparently the case with the pentacyanoferrate(II) species.¹¹ The absence of a statistical mixture is likely a consequence of the kinetic factors controlling the binding of each ruthenium pentaammine residue.

The ^1H NMR spectra of the $[\text{Ru}(\text{bpz})_3][\text{Ru}(\text{NH}_3)_5]_n^{(2+2n)+}$ complexes with $n = 0, 3$, and 6 are shown in Figure 5. For the $[\text{Ru}(\text{bpz})_3]^{2+}$ complex, the resonance signals observed at 10.05, 8.85, and 8.17 ppm were previously assigned to the H3, H5, and H6 protons, respectively. The NMR spectrum of the $[\text{Ru}(\text{bpz})_3][\text{Ru}(\text{NH}_3)_5]_3^{8+}$ complex does not seem to differ appreciably from the spectrum of the $[\text{Ru}(\text{bpz})_3]^{2+}$ cation. Given the close similarity in the spectra shown in Figure 5A,B and the small changes seen in the $\text{bpz}[\text{Ru}(\text{NH}_3)_5]_n$ system ($n = 1, 2$), with peripheral coordination, the assignment outlined in Table II is proposed. Any other assignment requires a substantial downfield shift in H6 or H6', which, again by analogy with the data in Figure 4, seems unlikely. In the case of the heptanuclear complex $[\text{Ru}(\text{bpz})_3][\text{Ru}(\text{NH}_3)_5]_6^{14+}$, the resonance signals at 9.96 (singlet), 8.83 (doublet), and 7.65 ppm (doublet) can be ascribed to the H3/H3', H5/H5', and H6/H6' protons, respectively.

Electrochemistry. Cyclic voltammograms of the $[\text{Ru}(\text{NH}_3)_5(\text{bpz})]^{2+}$ and $[\text{Ru}(\text{NH}_3)_5]_2(\text{bpz})^{4+}$ complexes can be seen in

Table II. Nuclear Magnetic Resonance Data

species	NMR spectral data ^a
bpz	9.46 (1) s [H3], 8.86 (2) s [H5, H6]
$\text{bpz}[\text{Ru}(\text{NH}_3)_5]^{2+}$	9.41 (2) d [H3, H3'], 8.83 (3) s [H5, H5', H6'], 8.27 (1) d [H6]
$\text{bpz}[\text{Ru}(\text{NH}_3)_5]_2^{4+}$	9.31 (2) s [H3, H3'], 8.75 (2) s [H5, H5'], 8.16 (2) d [H6, H6']
$[\text{Ru}(\text{bpz})_3]^{2+}$ (L)	10.05 (2) s [H3], 8.85 (2) d [H5], 8.17 (2) d [H6]
(L) $[\text{Ru}(\text{NH}_3)_5]_3^{8+}$	9.95 (2) m [H3, H3'], 8.8 (2) d [H5, H5'], 8.0 (2) m [H6, H6']
(L) $[\text{Ru}(\text{NH}_3)_5]_6^{14+}$	9.96 (2) s [H3, H3'], 8.83 (2) m [H5, H5'], 7.65 (2) m [H6, H6']

^aRelative intensities are given in parentheses. s = singlet; d = doublet; m = multiplet. See Figures 4 and 5 for numbering scheme. The $[\text{Ru}(\text{NH}_3)_5]^{2+}$ groups are coordinated by the unprimed numbered rings. See captions to Figures 4 and 5 for experimental conditions. L = $[\text{Ru}(\text{bpz})_3]^{2+}$.

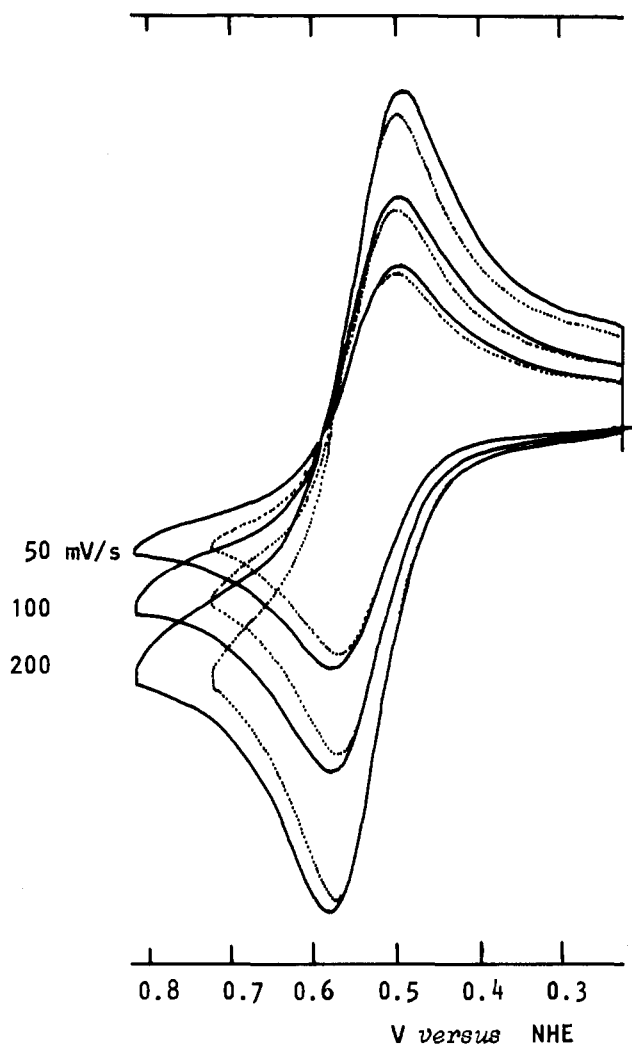


Figure 6. Cyclic voltammograms of $[\text{Ru}(\text{NH}_3)_5(\text{bpz})]^{2+}$ (---) (3 mM) and $[\text{Ru}(\text{NH}_3)_5]_2(\text{bpz})^{4+}$ (—) (1.5 mM) at several potential scan rates, in aqueous solution, with 0.10 M NaCl, at 25 $^\circ\text{C}$.

Figure 6. The voltammograms of the mononuclear complex follow very closely the several reversibility criteria based on the treatment of Nicholson and Shain,²⁶ with $E^\circ = 0.52$ V vs NHE and a diffusion coefficient of 2.5×10^{-6} $\text{cm}^2 \text{s}^{-1}$. The observed Ru(III)/Ru(II) potential is in the expected region.²⁷ In the case of the binuclear complex, only a single pair of cathodic and anodic waves is observed with a peak separation of 70 mV and $E^\circ = 0.53$

(26) Nicholson, R. S.; Shain, I. *Anal. Chem.* **1964**, *36*, 706.

(27) Curtis, J. C.; Sullivan, B. P.; Meyer, T. J. *Inorg. Chem.* **1983**, *22*, 224.

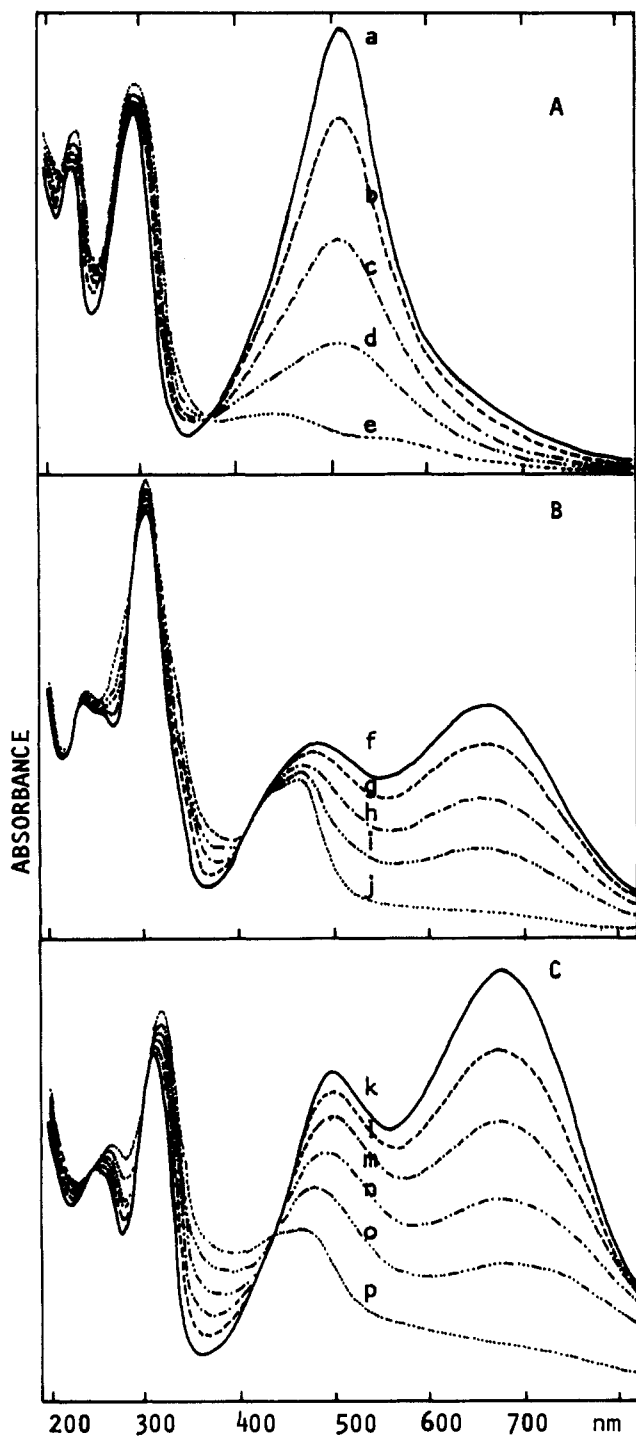


Figure 7. Spectroelectrochemistry of (A) $[\text{Ru}(\text{NH}_3)_5(\text{bpz})]^{4+}$ (1.3 mM), (B) $[\text{Ru}(\text{bpz})_3\text{Ru}(\text{NH}_3)_5]^{8+}$ (1.4 mM), and (C) $[\text{Ru}(\text{bpz})_3\text{Ru}(\text{NH}_3)_6]^{14+}$ (0.4 mM), in aqueous solution, with 0.10 M NaCl, at 25 °C: (a) 0, (b) 0.48, (c) 0.52, (d) 0.56, (e) 0.70, (f) 0, (g) 0.62, (h) 0.67, (i) 0.72, (j) 0.85, (k) 0, (l) 0.57, (m) 0.62, (n) 0.67, (o) 0.72, (p) 0.90 V vs NHE.

V. The voltammograms for the mononuclear and binuclear complexes normalized to constant $[\text{Ru}]$ are shown in Figure 6 and are very similar; however, the current profile is broader for the binuclear species than for the mononuclear species. As anticipated, the faradaic current is twice as large for the diruthenium species as for the monoruthenium species. The voltammogram of the binuclear complex can be simulated by a sum of two mono-electronic reversible waves, separated by approximately 0.01 V.

Spectroelectrochemical oxidation of the binuclear species proceeds as shown in Figure 7A with a formal potential of 0.52 V, leading to complete decay of the two $\text{Ru}_p(\pi) \rightarrow \text{bpz}(\pi^*)$ MLCT bands in the visible region. The Nernst slope of 70 mV is slightly

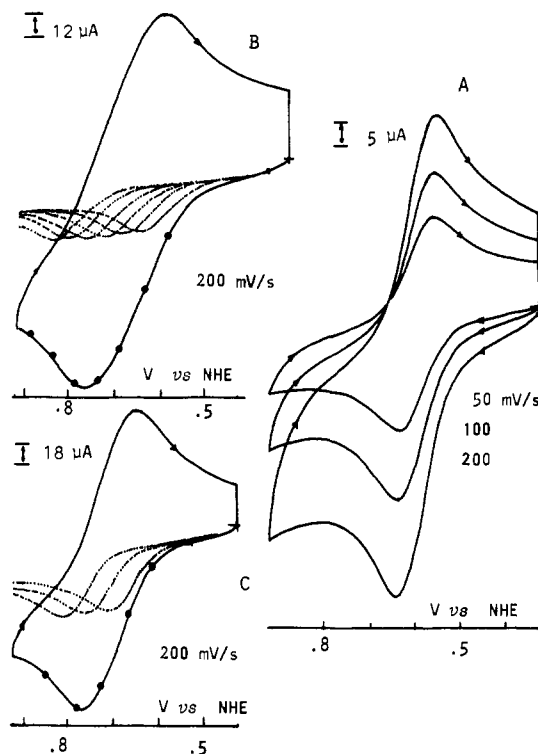


Figure 8. Cyclic voltammograms of the (A) 1:1, (B) 1:6, and (C) 1:3 tris(bipyrazine)ruthenium(II)–pentaammineruthenium(II) polynuclear complexes, 0.8, 0.6, and 1.0 mM, respectively, in aqueous solution, at 25 °C, with 0.10 M NaCl. Dotted lines refer to tentative deconvolution of the voltammograms in a series of reversible mono-electronic waves; black circles denote theoretical values.

higher than that expected for a reversible mono-electronic process (i.e. 59 mV) and is consistent with the occurrence of two successive steps having very similar E° . Measurements of the peripherally oxidized species in the near-IR region (800–1800 nm), in D_2O solutions, provided no evidence of low-energy intervalence-transfer (IT) transitions with $\epsilon > 100 \text{ M}^{-1} \text{ cm}^{-1}$.

Cyclic voltammograms of the $[\text{Ru}(\text{bpz})_3\text{Ru}(\text{NH}_3)_5]^{4+}$ complex in aqueous solution are shown in Figure 8A. The voltammograms are consistent with a reversible mono-electronic process, with $E^\circ = 0.69 \text{ V}$ and $D = 2.3 \times 10^{-6} \text{ cm}^2 \text{ s}^{-1}$. In the cases of the 1:3 and 1:6 polynuclear complexes, a pair of broad, quasi-reversible waves can be observed around 0.7 V in Figure 8B,C. The cathodic and anodic peaks are separated by almost 150 mV, having approximately 1:1 intensity ratio. The peak potentials do not vary with the potential scan rates in the range 20–200 mV s^{-1} . It seems probable that the large separation between the cathodic and anodic waves arises from the superimposition of several parallel mono-electronic processes having very close E° values. A quantitative simulation can be made, as in Figure 8B,C, by assuming a set of three reversible waves for the 1:3 complex, with $E^\circ = 0.67, 0.72,$ and 0.77 V ($D = 2.0 \times 10^{-6} \text{ cm}^2 \text{ s}^{-1}$), and a set of six reversible waves for the 1:6 complex, with $E^\circ = 0.62, 0.66, 0.70, 0.74, 0.78,$ and 0.82 V ($D = 1.4 \times 10^{-6} \text{ cm}^2 \text{ s}^{-1}$).

The spectroelectrochemistry of the $[\text{Ru}(\text{bpz})_3\text{Ru}(\text{NH}_3)_5]^{8+}$ and $[\text{Ru}(\text{bpz})_3\text{Ru}(\text{NH}_3)_6]^{14+}$ complexes in aqueous solution is illustrated in Figure 7B,C. The oxidation process leads to a decay of the $\text{Ru}_p \rightarrow \text{bpz}(\pi_1^*, \pi_2^*)$ bands in the visible region, indicating that the peripheral $[\text{Ru}(\text{NH}_3)_5]^{2+}$ groups are totally oxidized within a narrow range of potentials around 0.7 V. This result confirms the occurrence of the several parallel steps in the cyclic voltammograms. The spectra can be regenerated in more than 90% and 70% yields for the 1:3 and 1:6 complexes, respectively, by reduction at a potential just negative of 0.7 V. As expected, the corresponding Nernst slopes of 100 and 130 mV differ from that of a reversible mono-electronic process and are consistent with a series of parallel mono-electronic steps having very close E° values.

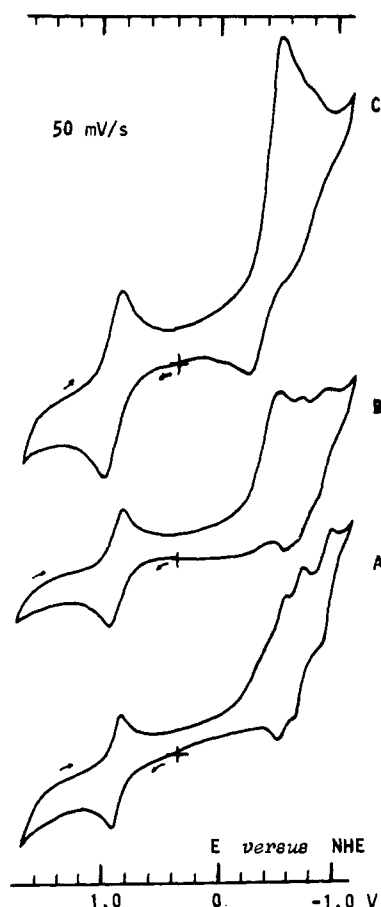


Figure 9. Cyclic voltammograms of the $[\text{Ru}(\text{bpz})_3\{\text{Ru}(\text{NH}_3)_5\}_n]^{(2+2n)+}$ complexes with (A) $n = 1$, (B) $n = 3$, and (C) $n = 6$, in acetonitrile (saturated solution) in the presence of 0.10 M tetraethylammonium hexafluorophosphate, at 25 °C.

The electronic spectra of the $[\text{Ru}^{\text{II}}(\text{bpz})_3\{\text{Ru}^{\text{III}}(\text{NH}_3)_5\}_n]^{(2+3n)+}$ complexes resemble that of the $[\text{Ru}(\text{bpz})_3]^{2+}$ cation, with an additional absorbance increase around 360 nm probably associated with LMCT transitions in the (N-heterocyclic) pentaammine-ruthenium(III) groups.^{28,29} Spectroelectrochemical measurements in the near-IR region (800–1800 nm), in D_2O solutions, provided no evidence of intervalence bands with $\epsilon > 100 \text{ M}^{-1} \text{ cm}^{-1}$. The possibility that the IT band is associated with the residual absorption around 700–800 nm, observed spectroelectrochemically, cannot be excluded. However, considering that minor, but detectable, amounts of decomposed oxidized products are always present in these systems, any assignment would be too speculative at the present stage.

Cyclic voltammograms in acetonitrile solutions are shown in Figure 9. The quasi-reversible waves associated with the $[\text{Ru}(\text{NH}_3)_5] \text{Ru}(\text{III})/\text{Ru}(\text{II})$ couples are similar to those measured in aqueous solution, except for an anodic shift of approximately 200 mV, which can be ascribed to solvent effects.²⁷ The several waves observed at -0.5 , -0.65 , and -0.9 V vs NHE for the $[\text{Ru}(\text{bpz})_3\{\text{Ru}(\text{NH}_3)_5\}_n]^{4+}$ complex are similar to those previously reported for the $[\text{Ru}(\text{bpz})_3]^{2+}$ cation³ and can be ascribed to the successive reduction of the bpz ligands. The electrochemical behavior becomes more complicated in the case of the 1:3 and 1:6 complexes, as shown in Figure 9B,C. However, this behavior is, in part, due to severe adsorption problems.

Concluding Remarks

The polynuclear $[\text{Ru}(\text{bpz})_3\{\text{Ru}(\text{NH}_3)_5\}_n]^{(2+2n)+}$ complexes represent an interesting, cubic-symmetry version of the linear-array $[(\text{NH}_3)_5\text{Ru}\{\text{pzRu}(\text{NH}_3)_4\}_n\text{pzRu}(\text{NH}_3)_5]^{(4+2n)+}$ ($n = 2-4$) com-

plexes studied by von Kameke, Tom, and Taube.³⁰ However, in contrast with the extended interactions observed in the linear systems, the peripheral $[\text{Ru}(\text{NH}_3)_5]^{2+}$ groups seem to be relatively isolated in the cubic complex. The energies of the MLCT bands and the electrochemical potentials for the $\text{Ru}(\text{III})/\text{Ru}(\text{II})$ couples vary only slightly with the number of $[\text{Ru}(\text{NH}_3)_5]^{2+}$ groups. No evidence of IT bands with $\epsilon > 100 \text{ M}^{-1} \text{ cm}^{-1}$ has been detected in the near-IR region, in contrast with the linear pyrazine-bridged systems and with Creutz and Taube's ion^{31,32} $[(\text{NH}_3)_5\text{Ru}-\text{pz}-\text{Ru}(\text{NH}_3)_5]^{5+}$. It is evident that up to six pentaammine-ruthenium(II) (or pentacyanoferrate(II)¹¹) groups may be coordinated by the $[\text{Ru}(\text{bpz})_3]^{2+}$ cation and that interaction between these groups is minimal. Surprisingly, the central $\text{Ru}_c(\pi) \rightarrow \text{bpz}(\pi^*)$ transition is also unaffected by such peripheral coordination, even when all the pentaammine groups are oxidized to $\text{Ru}(\text{III})$. This is contrary to the situation where the bpz rings are protonated,^{3b} in which case there is an effect upon the $\text{Ru}_c(\pi) \rightarrow \text{bpz}(\pi^*)$ transition energy. Lavallee and Fleischer²³ noted that the MLCT transitions of $\text{LRu}(\text{NH}_3)_5$ species ($L =$ a heterocyclic ligand) were linearly related to the redox potential $E(L/L^-)$ of the ligand L , where reduction occurs into the same orbital into which the electronic transition occurs. If we regard the unit $[\text{Ru}(\text{bpz})_3]^{2+}$ as a ligand toward $[\text{Ru}(\text{NH}_3)_5]^{2+}$, then we may add this datum point to the same graph, using the reduction potential for $[\text{Ru}(\text{bpz})_3]^{2+}$ instead of that for a simple ligand L . This extra datum point lies exceptionally well on the same line as the other ligands L but at very much more positive potential. The equation of this line for 11 points is

$$\nu(\text{CT}) = 0.51E(L/L^-) + 1.59 \text{ (in eV)} \quad (R = 0.98)$$

It is surely of considerable interest that the electronic spectra of these species are almost independent of the degree of peripheral binding, that each ruthenium pentaammine (or pentacyanoferrate) fragment is independent of the others, and further that the central ruthenium to bpz MLCT transition is independent of the extent of peripheral binding, even when the $[\text{Ru}(\text{NH}_3)_5]^{2+}$ groups are oxidized to $[\text{Ru}(\text{NH}_3)_5]^{3+}$. Recall that this is not true for binding of protons.^{3b} Expressed in another way, the several $[\text{Ru}(\text{NH}_3)_5]^{2+}$ groups generate several MLCT excited states that couple neither to each other nor to the central $[\text{Ru}^{\text{III}}_c(\text{bpz}^-)]$ excited MLCT state, at least on the time scale of absorption. Further, the $[\text{Ru}(\text{III})_p/\text{Ru}(\text{II})_n]$ couples appear identical, except for statistical effects, independent of the number of peripheral groups. Thus, the ground-state wave functions involving these groups are localized on each pyrazine ring. These results have considerable significance with respect to our understanding of the nature of charge-transfer states and their localization, delocalization, and emission. Possibly, each $\text{Ru}_p(\pi) \rightarrow \text{bpz}(\pi^*)$ transition is located within its own pyrazine ring and the transition is orthogonal to the central $\text{Ru}_c(\pi) \rightarrow \text{bpz}(\pi^*)$ transition, which, possibly, is localized in the diimine framework. Such diimine localization is consistent with the lack of a significant increase in the $\text{p}K_a$ value of the nitrogen atom trans to the ruthenium atom in the complexes $\text{bpz}[\text{Ru}(\text{NH}_3)_5]_n^{2n+}$ ($n = 1, 2$). However, resonance Raman data²² argue against this supposition.

Acknowledgment. Financial support from the FINEP and CNPq agencies in Brazil (H.E.T.), the Natural Sciences and Engineering Research Council of Canada (Ottawa), and the Office of Naval Research (Washington, DC) is gratefully acknowledged.

Registry No. $[\text{Ru}(\text{NH}_3)_5(\text{bpz})](\text{PF}_6)_2$, 111060-37-8; $[\text{Ru}(\text{NH}_3)_5(\text{bpz})]\text{Cl}_2$, 111060-44-7; $[\text{Ru}(\text{NH}_3)_5(\text{bpzH})]^{3+}$, 111085-45-1; $[\{\text{Ru}(\text{NH}_3)_5(\text{bpz})\}(\text{PF}_6)_4]$, 111085-44-0; $[\{\text{Ru}(\text{NH}_3)_5(\text{bpz})\}_2\text{Cl}_4]$, 111060-45-8; $[\{(\text{NH}_3)_5\text{Ru}\}_2(\text{bpzH})]^{5+}$, 111085-71-3; $[\text{Ru}(\text{NH}_3)_5(\text{H}_2\text{O})](\text{PF}_6)_2$, 34843-18-0; $[\text{Ru}(\text{bpz})_3\{\text{Ru}(\text{NH}_3)_5\}(\text{PF}_6)_4]$, 111060-39-0; $[\text{Ru}(\text{bpz})_3\{\text{Ru}(\text{NH}_3)_5\}_2\text{Cl}_4]$, 111060-46-9; $[\text{Ru}(\text{bpz})_3\{\text{Ru}(\text{NH}_3)_5\}_3](\text{PF}_6)_8$, 111060-41-4; $[\text{Ru}(\text{bpz})_3\{\text{Ru}(\text{NH}_3)_5\}_3]\text{Cl}_8$, 111060-47-0; $[\text{Ru}(\text{bpz})_3\{\text{Ru}(\text{NH}_3)_5\}_6](\text{PF}_6)_{14}$, 111060-43-6; $[\text{Ru}(\text{bpz})_3\{\text{Ru}(\text{NH}_3)_5\}_6]\text{Cl}_{14}$, 111060-48-1; $[\text{Ru}(\text{bpz})_3](\text{PF}_6)_2$, 80907-56-8.

(28) Gaunder, R.; Taube, H. *Inorg. Chem.* **1970**, *9*, 2627.

(29) Lever, A. B. P. *Inorganic Electronic Spectroscopy*, 2nd ed.; Elsevier: Amsterdam, 1984.

(30) Von Kameke, A.; Tom, G. M.; Taube, H. *Inorg. Chem.* **1978**, *17*, 1790.

(31) Creutz, C.; Taube, H. *J. Am. Chem. Soc.* **1969**, *91*, 3988.

(32) Creutz, C.; Taube, H. *J. Am. Chem. Soc.* **1973**, *95*, 1086.